

Move an Asteroid Competition 2019

Asteroid Control through Surface Restructuring

Manfred Ehresmann^{a,*}

^a *Institute of Space Systems, University of Stuttgart, Pfaffenwaldring 29, 70569 Stuttgart, Germany,*
ehresmann@irs.uni-stuttgart.de

** Corresponding Author*

Abstract

A novel concept of asteroid orbit control by restructuring asteroid surfaces to manipulate albedo and respective radiation pressure effects is introduced. The method itself is propellant less allowing for prolonged operation and permitting adaption and even reversing introduced reflection effects. Microscopic restructuring of asteroid surface material allows for the manipulation of reflective properties, which can be exploited for influencing orbit and attitude parameters. Asymmetric radiation pressures are well known for their ability to change the orbit of an asteroid through the Yarkovsky effect or rotational parameters by the YORP effect. In the simplest form albedo manipulation of an asteroid with a solid surface can be achieved with a single spacecraft mission. This spacecraft will locally focus energy from a very low (pseudo-)orbit onto the asteroids surface. The candidates for utilisation are CO₂ laser systems. First, conventionally laser engravers to brighten mineralic and metallic surfaces. Second, CO₂ laser cleaning systems often used to remove silicate residue of industrial processes.

It is calculated that an asteroid with a high albedo will experience significantly less Yarkovsky effect, resulting in reduced orbit drift and improved future predictability.

Laser technology can further be exploited to create surface structures that represent an asymmetric saw tooth pattern (i.e. repeating sharp right triangles) by using femto second laser pulses or by an angled focal point. This asymmetric surface pattern leads to an angular dependent reflectivity, which can be exploited to create radiation pressure differences. When properly applied, countering spin-rate changes and rotation axis drift of the YORP effect is possible. Preliminary analysis indicates feasibility for probes equipped with laser for treatment of Near Orth Objects.

Keywords: Asteroid, Planetary defense, Laser application, Yarkovsky effect

Nomenclature

A – area
A – albedo
 A_2 – asteroid physical parameter
a – acceleration
a – semi-major axis
 c_0 – vacuum light speed
 c_e – effective (exhaust) velocity
 Γ – thermal inertia
 γ – obliquity
d – model exponent
D – diameter
E – energy
 ϵ – emissivity
F – force
 Θ – thermal parameter
G – gravity constant
 G_S – solar constant
 m – mass
 \dot{m} – mass flow
n – multiplication factor
P – power
P – rotation period
p – semi latus rectum
 ρ – mass density

r – (radial) distance
 r_0 – mean distance of Earth
 S_A – projected area of sphere
 σ – Stefan-Boltzmann constant
t – time
 T_* – sub solar temperature
v – velocity
 Φ – standard radiation force factor

Acronyms/Abbreviations

AU – Astronomical Unit
IRS – Institute of Space Systems
LASER – Light Amplification by Stimulated Emission of Radiation
NASA – National Aeronautics and Space Administration
NEO – Near Earth-Object
US – United States
YORP – Yarkovsky-O’Keefe-Radzievskii-Paddack

1. Introduction

Planetary defence is literally a vital challenge for humankind. An impact with an asteroid of sufficient size has the capability for civilisation or world ending

scenarios. Destruction of an impact event is mainly caused by shock of wind, pressure, thermal radiation or tsunamis [1]. The primary hazards capable to trigger secondary effects like large-scale fires or secondary earthquakes, hindering emergency response efforts. The scale of destruction can very likely be beyond any national or even international relief efforts.

The current strategy for the threat of asteroids is therefore not focused on disaster response but on impact mitigation. The US ‘Nation near-Earth Object preparedness strategy and action plan’ summarizes five goals [2]. Four of these goals consider mitigation of an impact through enhanced observation, prediction, data exchange and development of appropriate mitigation and deflection technologies. While only the fifth goal considers the development and training with emergency protocols for minimizing direct harm.

The key to impact mitigation are technologies that enable the redirection or deflection of a large asteroid. Realistically the timespan for operating such a technology can be considered to be lengthy in application. As NASA states that the undertaking of an intercept mission, will require at least five years of preparation [3].

The NASA report “Near-Earth Object Survey and Deflection Analysis of Alternatives” [4] make the following assessments:

Nuclear standoff explosions are most likely highly effective in altering the trajectory and properties of a targeted - potentially harmful - asteroid but carry high development and operations risks. Especially the risk of fracturing an asteroid can lead to a hazardous cloud of asteroids fragments, which more likely of hitting Earth. Non-nuclear kinetic impactors are mature, but have a limited use-case against single small, solid asteroids. The alternative are “slow push” techniques, which are generally less mature and require long preparation times.

1.1. Slow Push Asteroid deflection techniques

A few examples of slow push techniques are given and briefly discussed:

1. The gravity tractor [5]:

The gravity interaction between an actively propelled spacecraft and the target asteroid is exploited for trajectory alteration. The applied force can directly be calculated with Newton’s law of universal gravitation [6]:

$$F = -G \frac{m_1 m_2}{r^2}, \quad (1)$$

Indicated by the universal gravitational constant of $G = 6.67408 \cdot 10^{-11} \text{ m}^3 \cdot \text{kg}^{-1} \text{ s}^{-2}$ [7], the resulting net force F between the two attracting masses m_1 and m_2 , with the distance r , will be very small for small celestial bodies and an orbiting space probe.

In principle, any probe with active propulsion can be utilized as gravity tractor and should be utilized in combination with other concepts given in the following.

2. Ion beam shepherd [8,9]:

An asteroid is exposed to a quasi-neutral plasma, which is then pushed into a desired direction. The generated force F upon the asteroid can then be calculated by:

$$F = n \dot{m} c_e, \quad (2)$$

Where the mass flow \dot{m} and the effective velocity c_e of the plasma and the coefficient n for adjusting between the cases of full absorption $n = 1$ and total reflection $n = 2$ of the impinging plasma particles.

Conventionally, electric propulsion systems require large power plants and have a very low mass flow producing very low thrust. While system with high mass flow have very high propellant consumption. Thus, applicability is very limited.

3. Laser ablation [10]:

Nearly indefinite operation can be achieved by using a high-power laser or other directed energy beam source to locally heat asteroid surface material above 3000 K for vaporization. Thus, an artificial thruster operated with ablated asteroid material is effectively created. The thrust can be calculated by Eqn. 2 with $n=1$, while the estimation of the thrust vector can be challenging, as laser ablation is not guaranteed to be uniform. Overall energy demand is high as mineral has to be heated above the required vaporization temperature.

4. White Painting [11,12]:

Changing the albedo of an asteroid allows for momentum exchange by photons of the sun. Thus, it has been proposed to whiten an asteroid through the application of white powders [11] or paint balls [12]. The main challenge here is, that the whitening agent has to be carried to the asteroid, budgeting the mass of a spacecraft. Thus, these concepts are likely to be bound for a single attempt due to mass constraints of the asteroid deflection space probe. The application of the agent might lead to stir up of dark surface dusts potentially negating or reducing the albedo enhancing effect.

In this paper, another concept is introduced combining the use of lasers for albedo changes. The use of a laser system does not require

additional mass that is consumed during operation. While laser operation can be quasi indefinite, allowing for more operational flexibility in terms of repeated irradiation and adapted patterns of surface (albedo) manipulation.

The power demand for such a system will be well below the power demand of a laser ablation system as no vaporization is required.

2. Assessment of radiation pressure effects

Photons have a mass through the fact that they store energy and can therefore exchange momentum when emitted, absorbed or reflected by or from an object. Although the generated force by these effects is small, it is a continuous force on celestial bodies perturbing their orbits.

The effect can be quickly estimated by considering the mass-energy equivalence:

$$E = mc_0^2 \quad (3)$$

and dividing by the time t to obtain a formulation for the radiation power P_{rad} yields:

$$\frac{E}{t} = P_{rad} = \dot{m}c_0^2, \quad (4)$$

which can be rearranged with $F = \dot{m} c_0$ to obtain

$$F = \frac{P_{rad}}{c_0} \quad (5)$$

When considering a single watt of absorbed radiation power the resulting force is $F_{1W,absorb} = 3.34 \text{ nN}$ and for full reflection $F_{1W,reflect} = 6.67 \text{ nN}$.

When considering full absorption on a square meter material and the solar constant of $G_S = 1371 \text{ W / m}^2$ is given by Eqn. 5 the resulting force can be calculated. The result is $F_{rad} = 4.5 \mu\text{N}$ with a vector radially outward from the Sun, fully agreeing with literature values using alternative derivations [13].

Asteroid trajectories are affected by radiation pressure of different origin. These effects and relevant equations are to be discussed in the following.

2.1. Solar radiation pressure

The solar radiation pressure results in a respective acceleration a_{srp} acting upon an asteroid. This force is calculated by the following equation [14, 15]:

$$a_{srp} = \frac{G_S S_A}{m_{astr} c_0} \left(1 + \frac{4}{9} A_{astr} \right) \left(\frac{r_0}{r} \right)^2. \quad (6)$$

Here the effectively radiated area S_A , the mass of the asteroid m_{astr} and the albedo of the asteroid A_{astr} are

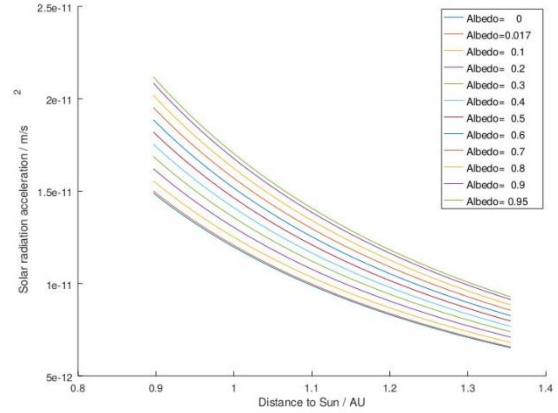


Figure 1: Radiation acceleration acting on asteroid Bennu in dependence of the distance from the sun for cases of varying albedo.

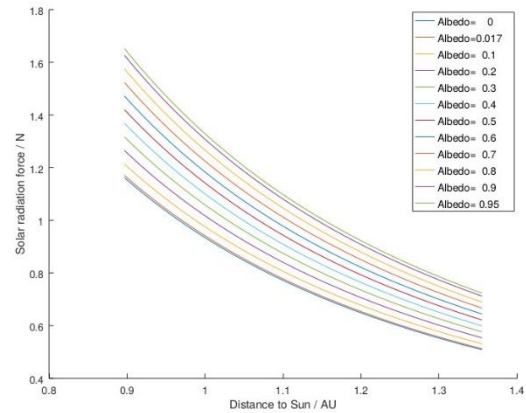


Figure 2: Radiation force acting on asteroid Bennu in dependence of the distance of the sun for cases of varying albedo.

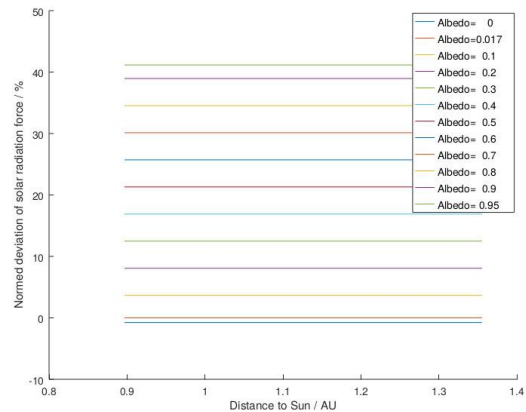


Figure 3: Relative radiation force acting on asteroid Bennu in dependence of the distance of the sun for cases of varying albedo. Comparing the force as a percentage difference from the force acting on Bennu with natural albedo of 0.017.

required as physical parameters. While the total received power is estimated through the distance square law, that considers the solar constant G_S , the mean distance of Earth to the sun r_0 to the actual distance r of the asteroid.

Table 1. Selected parameters of 101955 Benu relevant for the estimation of solar radiation pressure [14].

	101955 Benu
$A / -$	0.017
m / kg	$7.8 \cdot 10^{10}$
D / m	510
r_{peri} / AU	0.89674
r_{apo} / AU	1.3553
a / AU	1.126

* AU = Astronomical Unit = 149597900 km

2.1.1. Case Study: Asteroid 101955 Benu

To evaluate the effect of albedo change in the asteroid Benu the parameters in Table 1 are used.

The results are given in Fig. 1. to Fig. 3. The total solar radiation pressure is small, as it is on the order of 10^{-11} m/s², while the total force acting on the asteroid is estimated at approximately 1 N. Changing the albedo from the initial 0.017 of Benu allows for allows for a maximum increase of generated force by 41.2 % at an albedo of 95 % as shown in Fig. 3.

Simulations indicate that a maximum displacement of 18.2 km and reduction in the semi-major axis of 34 m is produced by this [14]. When naively assuming a linear correlation between acceleration and displacement a maximum position displacement of 25.7 km and a change of 48.11 m in the semi-major axis is achieved through solar radiation pressure, when increasing albedo. Thus, the overall effect in trajectory drift by solar radiation pressure in relation to albedo can be considered small.

2.2. Yarkovsky-effect

The Yarkovsky-effect describes asymmetric radiation of energy by a heated rotating body. A hot side emits more heat energy than a cold side; the total forces can be calculated by Eqn. 5, when respective emitted radiation powers are known.

For asteroids with spin-axis obliquity of near $\pm 180^\circ$ to the orbital plane, the hot side is rotated either into the direction of travel or behind it. Exerting a net force in prograde or retrograde direction, which is capable to significantly alter trajectories over time.

For simplicity reasons only a transversal Yarkovsky effect is considered in this paper, based on the model of [14]. Transversal Yarkovsky means that the force is generated in or against direction of travel.

For computing the transversal Yarkovsky acceleration, the following expression used [17]:

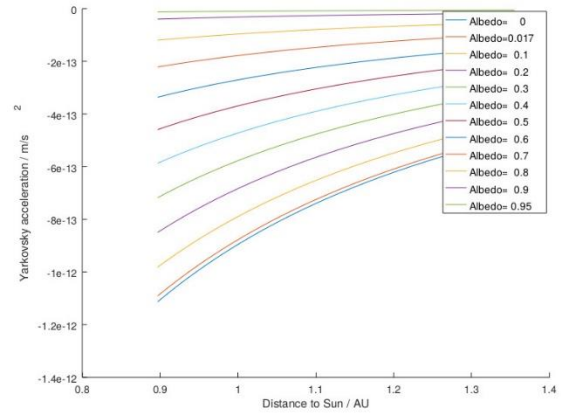


Figure 4: Yarkovsky acceleration acting transversal on asteroid Benu in dependence of the distance from the sun for cases of varying albedo.

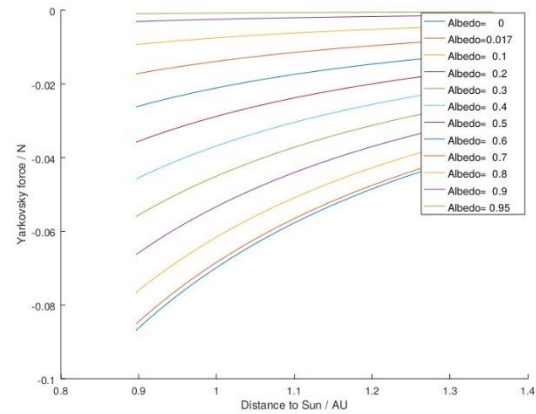


Figure 5: Yarkovsky force acting transversal on asteroid Benu in dependence of the distance from the sun for cases of varying albedo.

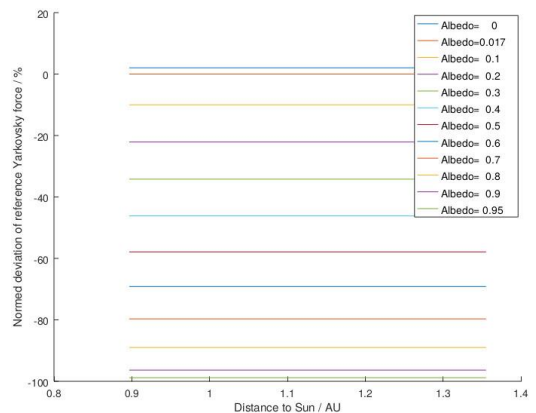


Figure 6: Relative Yarkovsky force acting transversal on asteroid Benu in dependence of the distance of the sun for cases of varying albedo. Comparing the force as a percentage difference from the force acting on Benu with natural albedo of 0.017.

$$a_{trans} = \left(\frac{r_0}{r}\right)^d A_2, \quad (7)$$

The constant $d = 2$ is utilized, which is 2-3 for most NEOs [18], resembling now the distance square law, with the reference distance of Earth r_0 and the current distance of the asteroid r .

The asteroid specific parameter A_2 is correlated to other physical parameters by [18, 19]:

$$A_2 = \frac{4(1-A)}{9} \Phi(1 \text{ AU}) f(\theta) \cos(\gamma), \quad (8)$$

where A is the asteroid bond albedo, which is the sum of reflection of all electromagnetic waves. The obliquity γ is the angle between the orbital plane normal axis and the rotation axis.

The standard radiation force factor at one astronomical unit is given by:

$$\Phi(1 \text{ AU}) = 3 \frac{G_S}{2 \rho D c_0}, \quad (9)$$

where the solar constant at G_S at 1 AU is correlated to the asteroid density ρ , the mean asteroid diameter D and the vacuum light speed c_0 .

The function of the thermal parameter is simply a product of linear heat theory and given as:

$$f(\theta) = \frac{1}{2} \frac{\theta}{1 + \theta + 0.5 \theta^2}, \quad (10)$$

The thermal parameter itself is defined as:

$$\theta = \frac{\Gamma}{\epsilon \sigma T_*^3} \sqrt{\frac{2\pi}{P}}. \quad (11)$$

With the thermal emissivity ϵ , the Stefan-Boltzmann constant σ , the thermal inertia Γ and the rotational period of the asteroid P .

The remaining parameter in Eqn. 11 is the subsolar Temperature T_* defined as:

$$T_* = \sqrt[4]{\frac{(1-A)G_S}{\epsilon \sigma p^2}}, \quad (12)$$

with already defined parameters except for the semi latus rectum p , given by:

$$p = a(1 - e^2), \quad (13)$$

with the orbital eccentricity e of the asteroid.

Table 2. Selected parameters of 101955 Benu relevant for the estimation of the Yarkovsky effect. [14]

101955 Benu

$d / -$	2
$\gamma / ^\circ$	175
$\rho / \text{kg/m}^3$	1260
$\epsilon / -$	0.9
$e / -$	0.9
$\Gamma / \text{J m}^{-1} \text{s}^{-\frac{1}{2}} \text{K}^{-1}$	310
P / h	4.29746

2.2.1. Case Study: Asteroid 101955 Benu

The data of Table 1 and Table 2 is used to assess the effects on asteroid Benu with varying Albedo. It is assumed that a change in bond albedo A does not affect the emissivity ϵ . The results of the respective transversal Yarkovsky acceleration, force and percentage deviation from the natural albedo are given in Fig. 4-6.

The total effect of force or acceleration shown in Fig. 4 and 5 vary by a factor of 2.28, achieving largest value closes to the sun and lowest values farthest from the sun. The total Yarkovsky acceleration and force of the asteroid Benu is smaller by two orders of magnitude, as for the case of natural bond albedo of 0.017 the acceleration is $\sim 10^{13} \text{ m/s}^2$ and $\sim 0.06 \text{ N}$.

This might appear to be a lower order effect than solar radiation pressure, but the transversal nature of the Yarkovsky effect does perturb the asteroid trajectory more severely.

Literature values for a 12-year propagation indicate that Yarkovsky forces produce a maximum displacement position of 185.20 km and a change in semi-major axis of 3.485 km [14]. Which is significantly more than the 18.2 km displacement and 0.034 change in semi-major axis for solar radiation pressure effects alone [14].

Figure 6 clearly shows that Yarkovsky forces and albedo have direct linear correlation, indicating that an increase in Albedo will at least linearly, more likely quadratic, reduce the perturbations caused of the Yarkovsky effect.

2.3. YORP-effect

The YORP-effect is a second order anisotropic radiation emission effect; it can be caused through asymmetric surface geometries or material properties [20]. The emission of a photon with a path deviating from the centre of gravity of the celestial body, causes either a torque or a force due to the momentum it carries with itself.

This change is small, as for example the observation of the asteroid 54509 YORP yielded that the spin rate will double in 600,000 years [21]. This drift varies the spin rate parameter P in Eqn. 11, ultimately changing the magnitude of the resulting Yarkovsky effect. The other perturbation produced by the YORP-effect is the spin-axis orientation changes by produced torques, changing the obliquity parameter γ in Eqn. 8. Making the order of magnitude and direction of the occurring Yarkovsky effect a prediction uncertainty. Modelling the magnitude

of the YORP effect is unfortunately beyond the scope of this work.

Selective albedo adaption of the asteroid surface is likely to mitigate the YORP effect, as here only minor changes of local albedo is required for more uniform radiation.

2.4. Conclusions on radiation effects.

The major radiation based orbit perturbation for most asteroids is the Yarkovsky effect. The considered example asteroid 101955 Bennu is representative of most asteroids with overall low bond albedo. Nonetheless, similar magnitudes of orbit perturbations are expected by other NEOs.

A reduction of the Yarkovsky effect by increasing the asteroid albedo allows for reducing orbit perturbation and improved predictability.

Localized albedo increase has the potential to minimize the YORP effect and therefore the drift of the Yarkovsky effect.

2.5. Potential mission scenario

A potential mission scenario with the aim of asteroid orbit stabilisation and potential deflection will follow two main operational phases:

1. Minimize YORP effect
 - a. Selectively albedo increase irregular surface geometries to obtain a quasi-uniform radiation pattern
 - b. Use incidence angle dependent reflectivity adaption by surface restructuring
2. Minimize Yarkovsky effect
 - a. Increase overall global albedo uniformly

An additional benefit of a mission scenario that overall increases bond albedo is the enhancement of remote observation of the treated asteroid.

3. Technology Assessment

The technology for manipulating asteroid albedo does already exist in multiple forms, while the quantitative analysis for this particular is not yet fully developed. Thus, indications for applicability and estimates for capabilities will be given in the following.

First, laser etching is commercially utilized technology to etch and mark a vast multitude of materials [22, 23]. Here the laser radiation causes the etched material to respond in a way to molecularly restructure its surface in a way that the incoming radiation is scattered more efficiently. Laser etching allows for effectively brightening the targeted material and increasing at least its geometric albedo, i.e. the diffuse reflection of incoming visible light.

The company Trotec gives the following list of etchable minerals: Granite, Marble, Slate, Basalt, Salt Crystals, Pebbles, Garden Stones, Stone Tiles, Natural Stone,

Ceramic / Porcelain [22]. These materials can be etched, i.e. brightened, with the use of CO₂ laser with output power of 12-120 W [23]. The list of laser treatable minerals can be extended by the large mineral group of silicates, as CO₂ lasers are used for laser cleaning of silicates [24, 25], indicating a strong susceptibility of this mineral group to CO₂ laser treatment.

It is further stated that:

“in general dark, regular stones are very well suited for engraving [...]. The surface of the stones does not have to be polished, natural stone structures are also well-suited to laser processing”. [26]

A sample of laser engraved slate is given in Fig. 7. Due to the lack of direct samples public available online imagery is used to albedo change estimation [22]. By using commercially available photo editing software it can be assessed that the brightness and therefore geometric albedo can be increased from at least 34 % up to 75 %, indicating a significant change in geometric albedo, which has to increase the bond albedo likewise.

If a new bond albedo of 50 % is assumed it can be compared to the data of relative Yarkovsky forces shown in Fig. 6. The result is that a relative reduction of Yarkovsky forces of 60 % is achieved; leading to significantly reduced orbital drift.

The second interesting technology is the utilisation of femto second laser pulses to generate micro structures that are capable to produce anisotropic reflectivity properties [27]. A simple geometric example of such a structure is given in Fig. 8.

Here it is shown that anisotropic reflective geometric



Figure 7: Sample of laser etched slate [22]. Significant change in albedo is evident, while digital measurement yield a maximum difference of 34 % to 75 % in brightness.

structures can be designed, where the angle of specular reflection is different for differing incidence angles of incoming radiation.

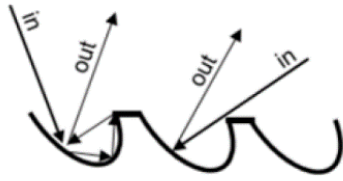


Figure 8: Example of an anisotropic reflection geometry [27].

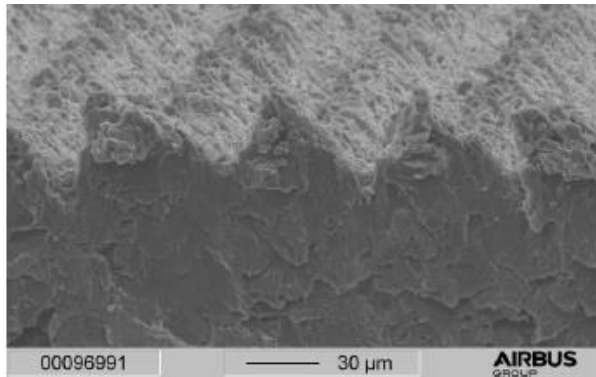


Figure 9: Example of laser treated aluminium, with anisotropic reflection microstructure [27].

The master thesis given in [27] was able to produce such microstructures with the use of femto second laser pulses and appropriate irradiation strategies as seen in Fig. 9. Such microstructures can be produced at least for the materials aluminium and titanium [27]. The brittle nature of minerals and behaviour of minerals when under the influence of laser cleaning devices indicates that microscopic chipping processes are likely to be achieved with femto second laser pulses as well.

Another key point of this technique is the reversibility of the applied surface effects, as by using the correct pulsing and overlap strategies of multiple passes, repeated whitening and darkening of surfaces is possible [27].

An extreme application of using incidence angle dependent reflectivity is given in Fig. 10. Here a maximum reflectivity or albedo is assumed for structures moving into the direction of the viewer, while structures moving away from the viewer have minimal reflectivity. This is an intended YORP effect, as this asymmetric reflectivity is a torque inducing asymmetry in radiation pressure. Over time, the rotation of the model object would slow down, stop and reverse – although such processes can take several hundreds to thousand years [21].

For a practical application, it can be expected that only localized micro restructuring is required to counter the YORP effect, as YORP torques and forces are caused by random structures and irregularities and are in total small.

3.1. Feasibility Analysis

For a preliminary feasibility assessment the asteroid Bennu is used again as a representative example, with a diameter of $D = 510 \text{ m}$, we can estimate a surface area of $A_{\text{Bennu,sphere}} = 8.2 \cdot 10^5 \text{ m}^2$ for a spherical shape. Thus, an additional 20 % margin is added to obtain the total area that is to be laser treated to be $A_{\text{Bennu}} = 9.9 \cdot 10^5 \text{ m}^2$.

Public sources indicate that commercially available CO₂ Laser can be operated for more than 50,000 h [25], allowing cumulative system operation for at least 5.7 years.

To allow for sufficient margin, the operative mission time is arbitrarily set to 3 years. Thus, the requirement for laser treating velocity per area becomes $\check{v}_{\text{surface}} = 0.01 \text{ m}^2/\text{s}$. Such a velocity might be achieved by adapting currently available systems, for example the Trotec Speedy series is qualified for movement speeds of up to $v_{\text{Trotec}} = 3.55 \frac{\text{m}}{\text{s}}$, when operating a CO₂ laser of at least 12 to 120 W [23]. As precision is not required for this application, a maximum diameter focal point or wide beam concept for effective engraving is desired.

The required beam width is simply calculated by dividing the area treatment speed by the movement speed and yields a required etching laser beam width of 2.8 mm to achieve the mission within the given 3-year range. Realizing such a laser is possible, when considering the wide beam laser cleaning systems with focal beams of 100 - 120 mm width that operate at a maximum of 1000 W of laser power [25].

A realistic estimate for the system can be produced by considering the minimal resolution of a speedy CO₂ engraving laser of 125 dpi [23]. This corresponds to a pixel size or beam width of 0.2 mm.

This laser beam diameter requires the stacking of 14

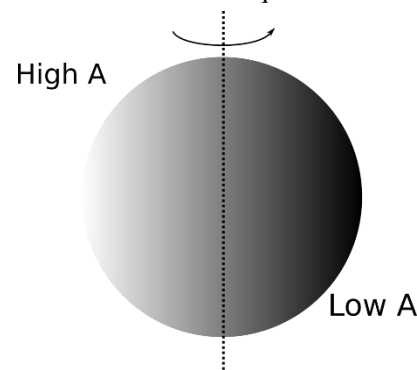


Figure 10: Example schematic of anisotropic reflectivity on a sphere to reduce rotation speed. Light source from the point of viewer. High reflectivity for incidence angle of 180° and low reflectivity for incidence angle of -180°

laser units to generate the respective line width. A single unit requiring $P_{\text{Laser}} = 12 - 120 \text{ W}$ each [23]. This

results in total laser output power of the modified system to be $P_{Laser,tot} = 168 - 1600$ W.

When considering a highly efficient system a CO₂ laser can have an efficiency of up to 20 % [29]. Thus, the resulting electric power system demand is 840 - 8400 W, while 672 - 6720 W of excess heat is generated, which has to be ultimately radiated away. Although these numbers are significant, they do indicate an overall technical feasibility.

A power demand for a worst-case assumption of 8.4 kW and a worst-case distance of the asteroid Bennu of 1.36 AU corresponds to an effective area of 9.2 m² of solar arrays, when considering 30 % efficiency for commercially available space grade photovoltaic cells [30]. This a feasible size for a solar array of an interplanetary probe. As a comparison, the Rosetta probe features 64 m² of solar panels [31].

Auxiliary systems for assessing and controlling the process should be based on the design of OSIRIS-Rex mission [32].

The following instruments are required for the success of the mission. A laser altimeter is required to determine the distance to the surface and adjust the laser focal beam accordingly. The bond albedo will be assessed by a sensor suite that records reflectivity on visible and infrared spectra as well as thermal emissions and adjusts irradiation strategies accordingly.

4. Conclusions & Outlook

This paper discussed whether it is possible to control an asteroid orbit by adjusting its albedo through surface restructuring. For this, the dependency of radiation driven orbit perturbations has been analysed. The considered effects are the solar radiation pressure and the Yarkovsky effect, while forces and accelerations for differing bond albedos have been calculated and resulting perturbations estimated. It was possible to show, that an increase in bond albedo allows for a significant reduction in orbit perturbation by the Yarkovsky effect, while a moderate perturbation by increased solar radiation pressure is generated.

Further, it was demonstrated that currently available laser etching technology is capable to produce the desired effect through the utilization of CO₂ laser systems. Sources indicate that laser etching technique is highly likely to be applicable to asteroid minerals of various nature.

An estimation was used to shown that it is possible that the full surface of the asteroid Bennu could be laser treated for albedo increase within 3 years of continuous operation within conventional mission design limitations. Faster mission times are possible; feasibility is directly correlated to the available electric power.

For further assessment of the presented concept, the following steps are recommended to further the maturity of the technology:

1. Higher order orbit perturbation assessment for a detailed quantitative analysis of orbit changes through albedo changes.
2. Experimental testing of achievable albedo change by laser etching of real or simulated asteroid material.
3. System analysis of laser etching devices in terms of mass, volume, heat, power and cost budgets.
4. Development of a designated laser-etching device for asteroid material for energy efficient area wide surface etching.
5. Preparation of a respective preparation/pathfinder mission.

5. Acknowledgement

The support of the interns Madleen Zipper and Jonathan Kurth, who aided in literature research and the implementation of relevant physical functions for the system design, is greatly acknowledged.

References

- [1] C. M. Rumpf, H. G. Lewis, P. M. Atkinson: Asteroid Impact Effects And Their Immediate Hazards For Human Populations Geophysical Research Letters, 2017, DOI: 10.1002/2017GL073191, <https://arxiv.org/abs/1703.07592v3>, last accessed 13.05.2019
- [2] National near-Earth object preparedness Strategy and Action Plan, Interagency Working Group for Detecting and Mitigating the Impact of Earth-bound near-Earth Objects, National Science & Technology Council, 2018 <https://www.whitehouse.gov/wp-content/uploads/2018/06/National-Near-Earth-Object-Preparedness-Strategy-and-Action-Plan-23-pages-1MB.pdf> , last accessed 13.05.2019
- [3] US Congress, Threats from Space: A Review of U.S. Government efforts to track and mitigate Asteroids and Meteors (Part I & Part II), Committee on Science, Space and Technology House of Representatives, 2013, <https://www.govinfo.gov/content/pkg/CHRG-113hrg80552/pdf/CHRG-113hrg80552.pdf>, last accessed 13.05.2019
- [4] NASA, Near-Earth Object Survey and Deflection Analysis of Alternatives, Report to Congress, 2007, https://www.nasa.gov/pdf/171331main_NEO_report_march07.pdf , last accessed 13.05.2019
- [5] E.T. Lu and S- G. Love: Gravitational tractor for towing asteroids, Nature, 2005, <https://arxiv.org/ftp/astro-ph/papers/0509/0509595.pdf>, last accessed 13.05.2019
- [6] Isaac Newton, Philosophiæ Naturalis Principia Mathematica, 1687
- [7] National Institute of Standards and Technology, Newtonian constant of gravitation,

- <https://physics.nist.gov/cgi-bin/cuu/Value?bg>, last accessed 13.05.2019
- [8] C. Bombardelli and J. Peláez: Ion Beam Shepherd for Asteroid Deflection, *Journal of Guidance, Control, and Dynamics*, 2011, <http://sdg.aero.upm.es/PUBLICATIONS/PDF/2011/AIAA-51640-157.pdf>, last accessed 13.05.2019
- [9] C. Bombardelli and J. Peláez: Ion Beam Shepherd for Contactless Space Debris Removal, *Journal of Guidance, Control, and Dynamics*, 2011, <http://sdg.aero.upm.es/PUBLICATIONS/PDF/2011/AIAA-51832-628.pdf>, last accessed 13.05.2019
- [10] P. Lubin, T. Brashears, G. Hughes, Q. Zhang, J. Griswald, K. Kosmo: Effective Planetary Defenseusing Directed EnergyDE-STARLITE. 14th IAA Planetary Defense Conference, 2015 <http://www.deepspace.ucsb.edu/wp-content/uploads/2013/09/PDC-2015-Lubin-e.pdf>, last accessed 13.05.2019
- [11] S. Ge, D. Hyland: Monte Carlo Simulations of Altering Yarkovsky Effect on the Near-Earth Asteroid Apophis via Deposition of Albedo Changing Powders, 2019, https://www.researchgate.net/publication/268290245_Monte_Carlo_Simulations_of_Altering_Yarkovsky_Effect_on_the_Near-Earth_Asteroid_Apophis_via_Deposition_of_Albedo_Changing_Powders, last accessed 13.05.2019
- [12] J. Chu: Paintballs may deflect an incoming asteroid, *MIT News*, 2012 <https://news.mit.edu/2012/deflecting-an-asteroid-with-paintballs-1026>, last accessed 13.05.2019
- [13] R. M. Georgevic: Mathematical Model of the Solar Radiation Force and Torques Acting on the Components of a Spacecraft, *Technical Memorandum* 33-494, 1971 <https://ntrs.nasa.gov/archive/nasa/casi.ntrs.nasa.gov/19720004068.pdf>, last accessed 13.05.2019
- [14] S. N. Deo, B.S. Kushvah: Yarkovsky effect and solar radiation pressure on the orbital dynamics of the asteroid (101955) Benu, *Astronomy and Computing*, Elsevier, 2017, <https://www.sciencedirect.com/science/article/pii/S213133716301330>, last accessed 13.05.2019
- [15] D. Vokrouhlický, A. Milani: 2000. Direct solar radiation pressure on the orbits of small near-Earth asteroids: Observable effects?. *Astronomy and Astrophysics*, 2000, https://www.researchgate.net/publication/234226003_Direct_solar_radiation_pressure_on_the_orbits_of_small_near-Earth_asteroids_Observable_effects, last accessed 13.05.2019
- [16] W. F. Bottke, D. Vokrouhlický, D. P. Rubincam, D. Nesvorný: The Yarkovsky and YORP Effects: Implications for Asteroid Dynamics. *Annual Review of Earth and Planetary Sciences*, 2006, https://www.boulder.swri.edu/~bottke/Reprints/Bottke_2006_Ann_Rev_Earth_Planet_34.157.Yarkovsky_YORP.pdf, last accessed 13.05.2019
- [17] S. R. Chesley, D. Farnocchia, M. C. Nolan, D. Vokrouhlický, P. W. Chodas, A. Milani, F. Spoto, B. Rozitis, L. A. M. Benner, W.F. Bottke, M. W. Busch, J. P. Emery, E. S. Howell, D. S. Lauretta, J.-L. Margot, P. A. Taylor: Orbit and bulk density of the OSIRIS-REx target Asteroid (101955) Benu. *Icarus*, 2014, <https://arxiv.org/pdf/1402.5573.pdf>, last accessed 13.05.2019
- [18] D. Vokrouhlický: Diurnal Yarkovsky effect as a source of mobility of meter-sized asteroidal fragments. I. Linear theory. *Astronomy and Astrophysics*. 335., 1998, <http://adsabs.harvard.edu/full/1998A%26A...335.1093V>, last accessed 13.05.2019
- [19] D. Farnocchia, S. R. Chesley, D. Vokrouhlický, A. Milani, F. Spoto: Near Earth Asteroids with measurable Yarkovsky effect, *Icarus*, 2018, <https://arxiv.org/pdf/1212.4812.pdf>, last accessed 13.05.2019
- [20] S. J. Paddack: Rotational bursting of small celestial bodies: Effects of radiation pressure. *Journal of Geophysical Research*. 1969
- [21] D. P. Rubincam, S. J. Paddack: As Tiny Worlds Turn, *Science*, 2007 <https://science.sciencemag.org/content/sci/316/5822/211.full.pdf>, last accessed 13.05.2019
- [22] trotec: Stone laser engraving, web page, <https://www.troteclaser.com/en/applications/stone/>, last accessed 13.05.2019
- [23] trotec: Profitability by design → Speedy, data sheet, https://www.troteclaser.com/fileadmin/content/images/Laser_Machines/Speedy_Series/laser-engraver-speedy-brochure.pdf, last accessed 13.05.2019
- [24] Clean Lasersysteme GmbH, Schweißnähte von Oxiden und Silikaten befreien, *Journal für Oberflächentechnik*, Springer, 2018, <https://link.springer.com/article/10.1007/s35144-018-0034-9>, last accessed 13.05.2019
- [25] p-laser: Low Power Control Unit General Design, web page, <https://www.p-laser.com/products/low-power>, last accessed 13.05.2019
- [26] trotec: Handbook for Engravers, manual, https://www.troteclaser.com/fileadmin/content/images/Contact_Support/Manuals/Handbook-for-engravers.pdf, last accessed 13.05.2019
- [27] M. P. Barrantes: Investigation for LASER based surface modification at different materials, IRS-18-S-018, Master thesis, Institute of Space Systems, University of Stuttgart, 2018
- [28] trotec: How to Choose the Right Resolution for your Engraving, web page, <https://www.troteclaser.com/en/knowledge/tips-for->

- [laser-users/resolution-laser-engraving/](#) , last accessed 13.05.2019
- [29] P.Vidaud, D.He, D.R.Hall: High efficiency RF excited CO2 laser, Optics Communications, Elsevier, 1985,
<https://www.sciencedirect.com/science/article/abs/pii/S0030401885901142>, last accessed 13.05.2019
- [30] azurspace: 30% Triple Junction GaAs Solar Cell, data sheet,
http://www.azurspace.com/images/0003429-01-01_DB_3G30C-Advanced.pdf, last accessed 13.05.2019
- [31] DLR: Rosetta at a glance - technical data and timeline, web page,
https://www.dlr.de/dlr/en/desktopdefault.aspx/tabid-10728/584_read-386/[https://www.dlr.de/dlr/en/desktopdefault.aspx/tabid-10728/584_read-386/](https://www.dlr.de/dlr/en/desktopdefault.aspx/tabid-10728/584_read-386) , last accessed 13.05.2019
- [32] NASA: OSIRIS-REx Asteroid Sample Return Mission, press kit, 2016,
https://www.nasa.gov/sites/default/files/atoms/files/osiris-rex_press_kit_0.pdf , last accessed 13.05.2019